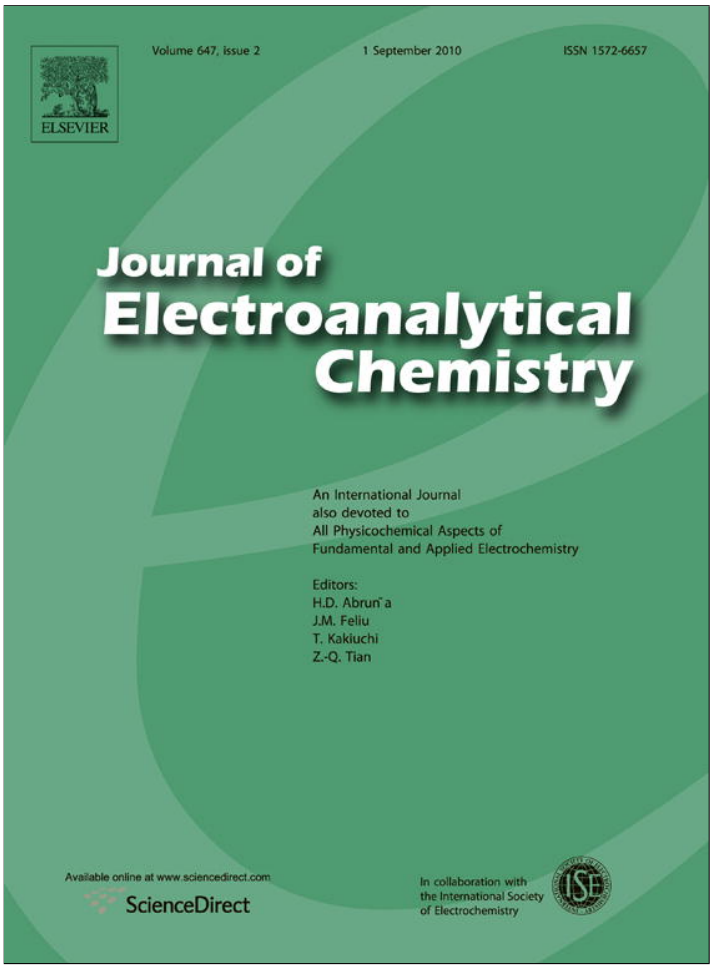

Journal of Electroanalytical Chemistry 647 (2010) 194–203

Contents lists available at ScienceDirect

Journal of Electroanalytical Chemistry

journal homepage: www.elsevier.com/locate/jelechem

Electrochemistry of substituted salen complexes of nickel(II): Nickel(I)-catalyzed reduction of alkyl and acetylenic halides

Matthew P. Foley [a], Peng Du [a], Kent J. Griffith [a], Jonathan A. Karty [a], Mohammad S. Mubarak [b], Krishnan Raghavachari [a], Dennis G. Peters [a,*]

[a] Department of Chemistry, Indiana University, Bloomington, IN 47405, USA
[b] Department of Chemistry, The University of Jordan, Amman 11942, Jordan

ARTICLE INFO

Article history:
Received 10 May 2010
Accepted 2 June 2010
Available online 9 June 2010

Keywords:
Catalytic reduction
Nickel salen complexes
Alkyl halides
Acetylenic halides
Intramolecular cyclization
Density functional theory

ABSTRACT

Dimethyl-, diethyl-, and diphenyl-substituted analogues of nickel(II) salen have been synthesized, and the cyclic voltammetric behavior of each compound at a glassy carbon electrode in dimethylformamide (DMF) containing tetra-*n*-butylammonium tetrafluoroborate ($TBABF_4$) has been compared with that of nickel(II) salen itself. Differences in the cathodic peak potentials for these species have been rationalized with the aid of theoretical computations based on density functional theory. Cyclic voltammograms for reduction of dimethylated nickel(II) salen reveal that placing a methyl group on the carbon atom of each imino (C=N) bond of the ligand improves the performance of electrogenerated dimethylated nickel(I) salen as a catalyst for reduction of 1-iodobutane. This conclusion is supported by experiments that combine controlled-potential electrolysis with high-performance liquid chromatography–electrospray ionization–mass spectrometry (HPLC–ESI–MS) to detect and analyze the post-electrolysis nickel-containing species arising from the bulk catalytic reduction of 1-iodooctane. Additional studies have been made of the use of electrogenerated dimethylated nickel(I) salen for the catalytic reduction of alkyl halides and for the reductive intramolecular cyclization of acetylenic halides.

1. Introduction

Electrogenerated nickel(I) complexes have been used extensively as catalysts for the reductive cleavage of carbon–halogen bonds in a wide variety of organic compounds. In a recent paper [1] from our laboratory, we provided a listing of 61 reports on this topic that were published between 1978 and 2006. Subsequent research in this field includes studies of nickel(I) tetramethylcyclam-catalyzed intramolecular cyclizations of propargyloxy and allyloxy α-bromoesters in both ethanolic media [2,3] and microemulsions [4], of propargyl bromoethers in dimethylformamide (DMF) [5], and of unsaturated organic halides in both aprotic and protic media [6]. In addition, three different electrogenerated nickel(I) complexes have been employed in DMF and in ethanol to effect the catalytic reductive intramolecular cyclization of *N*-allyl-α-haloamides to afford pyrrolidinones [7]. A recent review [8] has surveyed the field of environmentally friendly, electrochemically based intramolecular cyclizations, many of which involve the use of nickel(I) catalysts. Much of our own research in this field, summarized elsewhere [1], has focused on electrogenerated [[2,2′-[1,2-ethanediylbis(nitrilomethylidyne)]bis[phenolato]]-*N*,*N*′,*O*,*O*′]nickelate(I), better known as nickel(I) salen, as a catalyst, mainly in homogeneous media but occasionally immobilized within a polymer film on an electrode surface, for the reduction of halogenated organic species. Examples of more recent work in our laboratory are the nickel(I)-catalyzed reductive intramolecular cyclization of some phenyl-conjugated acetylenic halides [9] and the nickel(I) salen-promoted ring-expansion reactions of 1-haloalkyl-2-oxocycloalkanecarboxylates [10].

We became intrigued by an account published by Miranda, Wade, and Little [11], in which an electrochemically reduced form of nickel(II) salen was employed catalytically to produce (*R*)-methyl 2-(2-hydroxycyclohexyl)acetate via the intramolecular cyclization of (*E*)-methyl 8-oxooct-2-enoate. These workers proposed a set of mechanistic pathways in which (i) nickel(II) salen undergoes a ligand-centered, one-electron reduction of an imino (C=N) bond, (ii) a molecule of substrate docks with the negatively charged carbon atom of the reduced imino bond, (iii) electron transfer to the docked substrate occurs, and (iv) reduced substrate undocks from the catalyst (which is converted back to nickel(II) salen) and undergoes intramolecular cyclization. To substantiate this mechanism, Miranda and co-workers synthesized a dimethylated version of nickel(II) salen by substituting a methyl group for the hydrogen atom on each imino carbon atom of the ligand. When

* Corresponding author. Tel.: +1 812 855 9671; fax: +1 812 855 8300.
E-mail address: peters@indiana.edu (D.G. Peters).

1572-6657/$ - see front matter © 2010 Elsevier B.V. All rights reserved.
doi:10.1016/j.jelechem.2010.06.001

this dimethylated nickel(II) salen was electrochemically reduced, it did not promote any formation of the desired cyclic product, an observation leading to the conclusion that the methyl groups congest the region of the complex where docking of the substrate would take place, thereby preventing the dimethylated nickel(I) salen from interacting with the substrate.

In view of our research [12] dealing with insertion of alkyl groups into the imino bonds of the salen ligand that takes place during the nickel(I)-catalyzed electrochemical reduction of alkyl halides and that decreases the efficiency of the catalytic process, we wondered whether placing sterically bulky substituents on the imino carbon atoms of the ligand would improve the performance of these electrogenerated nickel(I) species. Accordingly, in the present work, we have synthesized the dimethyl-, diethyl-, and diphenyl-substituted analogues of nickel(II) salen by replacing the hydrogen atom of each imino carbon atom of the ligand with a methyl, ethyl, or phenyl moiety. We have employed cyclic voltammetry (i) to investigate the reversible, one-electron reduction of each of the substituted nickel(II) salens at glassy carbon electrodes in DMF containing tetraalkylammonium tetrafluoroborates, (ii) to compare the electrochemistry of each disubstituted compound with respect to nickel(II) salen itself, and (iii) to examine the catalytic reduction of 1-iodobutane by each electrogenerated nickel(I) species. In addition, we have carried out theoretical calculations based on density functional theory to correlate the predicted energy states for the various nickel(II) and nickel(I) species with experimentally measured cathodic peak potentials for the one-electron reduction of each nickel(II) complex. High-performance liquid chromatography–electrospray ionization–mass spectrometry (HPLC–ESI–MS) has been used to demonstrate that, during the catalytic reduction of 1-iodooctane by electrogenerated dimethylated nickel(I) salen, the presence of a relatively bulky methyl group (instead of a hydrogen atom) on each imino carbon atom of the ligand does indeed block octylation of the imino bond of the ligand almost completely, thereby enhancing the integrity of the dimethyl-substituted complex as a catalyst in comparison with nickel(I) salen itself. Finally, we have explored the use of electrogenerated dimethylated nickel(I) salen as a catalyst for the preparative-scale reduction of several alkyl and acetylenic halides. Product distributions arising from these controlled-potential (bulk) electrolyses have been determined with the aid of gas chromatography–mass spectrometry (GC–MS), and a set of mechanistic pathways has been formulated to describe the observed catalytic processes.

2. Experimental

2.1. Reagents

Each of the following reagents was purchased from Aldrich Chemical Company and was used as received: [[2,2′-[1,2-ethanediylbis(nitrilomethylidyne)]bis[phenolato]]-*N*,*N*′,*O*,*O*′]nickel(II) (hereafter referred to as nickel(II) salen, 98%), 1-(2-hydroxyphenyl)ethanone (99%), 1-(2-hydroxyphenyl)propan-1-one (97%), (2-hydroxyphenyl)(phenyl)methanone (99%), *n*-butyllithium (1.6 M in hexanes), *tert*-butyllithium (1.7 M in pentane), 1,4-dibromobutane (99%), 1,4-diiodobutane (99%), phenylacetylene (98%), tri-*n*-butyltin hydride (97%), 2,2′-azobis(2-methylpropionitrile) (AIBN, 98%), 1-hexyne (97%), 1-bromobutane (99%), 1-iodobutane (99%), 1-iodooctane (98%), *n*-dodecane (99%), *n*-hexadecane (99%), *n*-nonane (99%), 1-octene (98%), and *n*-octane (99%). Other chemicals, used as received, were ammonium acetate (EM Science, ACS reagent grade), 1-bromooctane (Baker), ethanol (Pharmco-Aaper, 200 proof), 5-decyne (Acros, 99%), diethylamine (Fisher, ACS reagent grade), ethylenediamine (Fisher, >98%), and nickel(II) acetate tetrahydrate (Fisher, ACS reagent grade). Dimethylformamide (DMF, Fisher Scientific, certified ACS grade) was used as the solvent for all electrochemical experiments. Tetramethylammonium tetrafluoroborate ($TMABF_4$) was recrystallized from water–methanol, and tetra-*n*-butylammonium tetrafluoroborate ($TBABF_4$) was recrystallized from ethyl acetate–pentane; after being recrystallized, these electrolytes (originally 98% pure, as purchased from GFS Chemicals) were stored in a vacuum oven at 75 °C prior to use. Tetrahydrofuran (THF, Mallinckrodt, ACS certified, >99.8%), used as a solvent in the syntheses outlined below, was dried in a water-removal system prior to use.

2.2. Synthesis of substituted salen ligands

Three different substituted salen ligands (**2a**–**c**) were prepared by means of the following general reaction [13]:

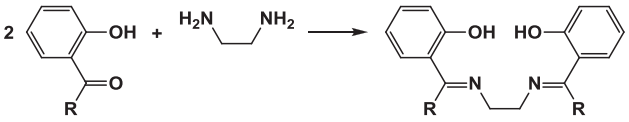

1a: R = CH_3
1b: R = C_2H_5
1c: R = C_6H_5

2a: R = CH_3
2b: R = C_2H_5
2c: R = C_6H_5

Ethylenediamine was added to stirred ethanolic solutions of 1-(2-hydroxyphenyl)ethanone (**1a**), 1-(2-hydroxyphenyl)propan-1-one (**1b**), and (2-hydroxyphenyl)(phenyl)methanone (**1c**); in each case, the molar ratio of diamine to ketone was 2:1. Each reaction mixture was heated to reflux for a minimum of 30 min. When the solutions were cooled to room temperature, bright yellow precipitates of **2a** and **2b** were obtained and an orange precipitate of **2c** was formed. After being collected by means of cold vacuum filtration, each solid was washed with cold ethanol to remove any unreacted starting materials, and the ligands were dried in air. Product identity was confirmed with the aid of electrospray ionization–mass spectrometry (ESI–MS) and ^1H NMR spectroscopy (300-MHz Varian Gemini 2000 instrument: (a) for **2a**, *m*/*z* (70 eV) 297 $[M+H]^+$; ^1H NMR ($CDCl_3$) δ 7.52–6.70 (8H), 3.99 (s, $-CH_2-N{=}C-$, 4H), 2.39 (s, $CH_3-C{=}N-$, 6H); (b) for **2b**, *m*/*z* (70 eV) 325 $[M+H]^+$; ^1H NMR ($CDCl_3$) δ 7.52–6.70 (8H), 3.98 (s, $-CH_2-N{=}C-$, 4H), 2.82 (q, $CH_3-\mathbf{CH_2}-C{=}N-$, 6H), 2.82 (t, $\mathbf{CH_3}-CH_2-$, 6H); for **2c**, *m*/*z* (70 eV) 421 $[M+H]^+$; ^1H NMR ($CDCl_3$) δ 6.6–7.7 (18H), 3.70 (t, $N-CH_2-$, 4H); NMR signals for the hydroxyl protons of the three ligands were not detected due to exchange with traces of water in the $CDCl_3$ solvent.

2.3. Metallation of the ligands

Metallation of the ligands to form the desired nickel(II) complexes (**3a**–**c**) was accomplished by addition of a stoichiometric quantity of nickel(II) acetate tetrahydrate dissolved in water to an ethanolic solution of the appropriate ligand [13]:

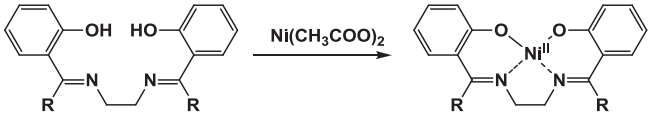

2a: R = CH_3
2b: R = C_2H_5
2c: R = C_6H_5

3a: R = CH_3
3b: R = C_2H_5
3c: R = C_6H_5

When the nickel(II) salt was added, the color of the solution changed from bright yellow (or orange) to red as nickel(II) was chelated by the ligand. Crystals were collected with the aid of cold vacuum filtration, were washed with cold ethanol, and were dried in a vacuum oven (3 torr, 75 °C) for at least 24 h. To confirm the identity of each nickel(II) complex, high-resolution mass spectral (HRMS) data were acquired with the aid of a Thermo Electron Corporation MAT 95XP-Trap instrument: (a) for **3a**, *m*/*z*: calcd.

for $C_{18}H_{18}N_2O_2{}^{58}Ni$ $[M]^+$ 352.0722, found 352.0724; calcd. for $C_{18}H_{18}N_2O_2{}^{60}Ni$ $[M]^+$ 354.0676, found 354.0699; calcd. for $C_{18}H_{18}N_2O_2{}^{61}Ni$ $[M]^+$ 355.0679, found 355.0746; calcd. for $C_{18}H_{18}N_2O_2{}^{62}Ni$ $[M]^+$ 356.0652, found 356.0690; calcd. for $C_{18}H_{18}N_2O_2{}^{64}Ni$ $[M]^+$ 358.0648, found 358.0574; for **3b**, *m*/*z*: calcd. for $C_{20}H_{22}N_2O_2{}^{58}Ni$ $[M]^+$ 380.1035, found 380.1026; calcd. for $C_{20}H_{22}N_2O_2{}^{60}Ni$ $[M]^+$ 382.0989, found 382.0996; calcd. for $C_{20}H_{22}N_2O_2{}^{61}Ni$ $[M]^+$ 383.0992, found 383.1021; calcd. for $C_{20}H_{22}N_2O_2{}^{62}Ni$ $[M]^+$ 384.0965, found 384.1001; calcd. for $C_{20}H_{22}N_2O_2{}^{64}Ni$ $[M]^+$ 386.0961, found 386.1000; for **3c**, *m*/*z*: calcd. for $C_{28}H_{22}N_2O_2{}^{58}Ni$ $[M]^+$ 476.1035, found 476.1041; calcd. for $C_{28}H_{22}N_2O_2{}^{60}Ni$ $[M]^+$ 478.0989, found 478.1058; calcd. for $C_{28}H_{22}N_2O_2{}^{61}Ni$ $[M]^+$ 479.0992, found 479.1099; calcd. for $C_{28}H_{22}N_2O_2{}^{62}Ni$ $[M]^+$ 480.0965, found 480.1088; calcd. for $C_{28}H_{22}N_2O_2{}^{64}Ni$ $[M]^+$ 482.0961, found 482.0956.

2.4. Syntheses of acetylenic halides

Previously published procedures [14–16] were modified for the preparation of 1-bromo-5-decyne and 1-iodo-5-decyne. To a solution of 1-hexyne in dry THF was added 1.6 M *n*-butyllithium in hexanes, and the mixture was heated at reflux for at least 2 h. After the reaction mixture was cooled to room temperature, the appropriate amount of 1,4-dihalobutane was added, and the system was kept at refluxing temperature overnight. Next, the mixture was cooled to room temperature, and the reaction was quenched by the addition of water (2 mL). Then the reaction mixture was filtered to remove solids, and the filtrate was concentrated under reduced pressure. Finally, each desired product was purified by elution through a silica gel column, and GC–MS and ^{1}H NMR spectrometry were employed to verify the identities of these materials: (a) for 1-bromo-5-decyne, *m*/*z* (70 eV) 218, M^+; 216, M^+; 137, $[M-Br]^+$; 95, $[M-C_3H_6Br]^+$; ^{1}H NMR ($CDCl_3$) δ 3.21 (t, CH_2Br, 2H); 2.18 (m, CH_2–C≡C–CH_2, 4H); 1.98 (quintet, C**H$_2$**–CH_2Br, 2H); 1.58 (m, C**H$_2$**–CH_2–C≡C, 4H); 1.42 (m, C**H$_2$**–CH_3, 2H); 0.91 (t, CH_3, 3H); (b) for 1-iodo-5-decyne, *m*/*z* (70 eV) 264, M^+; 137 $[M-I]^+$; 95 $[M-C_3H_6I]^+$; ^{1}H NMR ($CDCl_3$) δ 3.21 (t, CH_2I, 2H), 2.16 (m, CH_2–C≡C–CH_2, 4H), 1.97 (quintet, C**H$_2$**–CH_2I, 2H), 1.58 (m, C**H$_2$**–CH_2–C≡C, 4H), 1.42 (m, C**H$_2$**–CH_3, 2H), 0.91 (t, CH_3, 3H).

Synthesis of 6-bromo-1-phenyl-1-hexyne was carried out according to a literature-based protocol [17]. To a solution of lithium phenylacetylide (obtained from the reaction of *n*-butyllithium with phenylacetylene in freshly distilled tetrahydrofuran) was added a stoichiometric quantity of 1,4-dibromobutane, and the reaction mixture was heated at reflux overnight. After being cooled to room temperature, the mixture was treated with water (2 mL), and the organic phase was dried over anhydrous magnesium sulfate and was subjected to rotary evaporation to remove volatile solvent. Finally, the residue was vacuum distilled (103 °C at 0.1 torr) to afford 6-bromo-1-phenyl-1-hexyne as a clear liquid, the identity of which was confirmed by means of GC–MS and ^{1}H NMR data: *m*/*z* (70 eV) 238, M^+; 236, M^+; 157, $[M-Br]^+$; 129, $[M-C_2H_4Br]^+$; 115, $[M-C_3H_6Br]^+$; 91, $[M-C_5H_6Br]^+$; 77, $[M-C_6H_8Br]^+$; ^{1}H NMR ($CDCl_3$) δ 7.33 (m, C_6H_5, 5H), 3.45 (t, CH_2Br, 2H), 2.39 (t, C≡CCH_2, 2H), 1.5–2.3 (m, CH_2, 4H).

2.5. Syntheses of carbocyclic electrolysis products

Pentylidenecyclopentane was prepared according to a previously published procedure [14,16]. A solution of 1-bromo-5-decyne, tri-*n*-butyltin hydride, and 1.8 mol% of 2,2′-azobis(2-methylpropionitrile) (AIBN) in benzene was refluxed for 36 h, after which the product was purified by reduced-pressure distillation (50 °C at 4 torr) and its identity was confirmed with the aid of GC–MS and ^{1}H NMR data: *m*/*z* (70 eV) 138, M^+; 123, $[M-CH_3]^+$; 109, $[M-C_2H_5]^+$; 95 $[M-C_3H_7]^+$; ^{1}H NMR (CCl_4) δ 5.13 (m, C=CH, 1H), 2.13 (m, CH_2C=C, 6H), 1.3–1.6 (m, CH_2, 8H), 0.89 (t, CH_3, 3H).

Benzylidenecyclopentane and (cyclopentenylmethyl)benzene were synthesized by means of a procedure reported by Michaely [18,19]. To a solution of cyclopentyllithium, prepared via the reaction between cyclopentyl bromide and lithium wire in dry tetrahydrofuran and cooled in an ice bath under argon, freshly distilled benzaldehyde was slowly added, and the resulting solution was stirred for 1 h. A saturated aqueous solution of ammonium chloride was added, and the organic phase was washed with water and dried over anhydrous magnesium sulfate; removal of the solvent by means of rotary evaporation gave crude cyclopentylphenyl carbinol. After the cyclopentylphenyl carbinol was dissolved in dry diethyl ether and this solution was placed in an ice bath, pyridine and thionyl chloride were added and the mixture was stirred for 1 h, after which water was slowly introduced. Next, the organic phase was separated and washed successively with dilute hydrochloric acid, saturated aqueous sodium bicarbonate, and water. Finally, the ether phase was dried and concentrated, and the residue was distilled to give an approximately 40:60 mixture of benzylidenecyclopentane and (cyclopentenylmethyl)benzene, which are separable by means of preparative-scale gas chromatography. These two compounds were characterized with the aid of GC–MS and ^{1}H NMR spectrometry: (a) for benzylidenecyclopentane, *m*/*z* (70 eV) 158, M^+; 129, $[M-C_2H_5]^+$; 117, $[M-C_3H_5]^+$; 91, $C_7H_7{}^+$; 67, $[M-C_7H_7]^+$; ^{1}H NMR ($CDCl_3$) δ 7.28 (m, C_6H_5, 5H), 6.34 (m, vinylic H, 1H), 2.50 (m, allylic H, 4H), 1.74 (m, CH_2, 4H); (b) for (cyclopentenylmethyl)benzene, *m*/*z* (70 eV) 158, M^+; 129, $[M-C_2H_5]^+$; 117, $[M-C_3H_5]^+$; 91, $C_7H_7{}^+$; 67, $[M-C_7H_7]^+$; ^{1}H NMR (CCl_4) δ 7.13 (m, C_6H_5, 5H), 5.31 (m, vinylic H, 1H), 3.34 (m, benzylic H, 2H), 1.4–2.6 (m, CH_2, 6H).

2.6. Instrumentation, cells, and electrodes

Cells and instrumentation for cyclic voltammetry and controlled-potential (bulk) electrolysis have been previously described [20,21]. For cyclic voltammetry the working electrode consisted of a short length of 3-mm-diameter glassy carbon rod (Tokai Electrode Manufacturing Co., Tokyo, Japan, Grade GC-20) press-fitted into a Teflon sleeve to provide a circular, planar surface with a geometric area of 0.077 cm^2. Before each experiment the electrode was polished with an aqueous suspension of 0.05-μm alumina (Buehler) on a Master-Tex (Buehler) polishing pad. After the electrode was polished, it was rinsed with distilled water, blotted dry with a Kim-Wipe, placed in an ultrasonic bath in contact with DMF for at least 30 s, and blotted dry with a Kim-Wipe. Working electrodes for controlled-potential (bulk) electrolyses were reticulated vitreous carbon discs (RVC 2X1-100S, Energy Research and Generation, Inc., Oakland, CA), approximately 3.7 cm in diameter, 0.5 cm in thickness, and 200 cm^2 in surface area) that were cut from longer rods. Procedures for fabricating, cleaning, and handling of these electrodes were taken from previously published work [21].

Solutions used for the various electrochemical experiments were deoxygenated with ultrahigh purity argon (Matheson Tri Gas) for a minimum of 10 min and were kept under an argon atmosphere during data collection. Cyclic voltammograms were acquired with the aid of (a) an in-house built linear-sweep potentiostat connected to a computer running internally written software, (b) a Princeton Applied Research Corporation (PARC) model 273A potentiostat–galvanostat operated by PARC Research Electrochemistry Software 4.30, (c) an Obbligato Objectives, Inc., Faraday MP potentiostat running Faraday MP version 1.5 software with data processing either in Excel or Origin, or (d) a PARC 2273 instrument running PowerSuite® software (PowerSuite®–2.58, PowerSuite® I/O Library–2.43.0, and PowerCV®–2.41). Controlled-

potential (bulk) electrolyses were conducted with (a) a PARC model 173 potentiostat–galvanostat connected to a computer running internally written software or (b) a PARC model 2273 instrument running PowerSuite® software (PowerSuite®–2.58, PowerSuite® I/O Library–2.43.0, and PowerSTEP®–2.41). Coulometric *n* values acquired with the aid of PowerSTEP®–2.41 software may suffer from the way in which data files are managed by the program. This software prepares a database file to collect 3000 data points (*I* versus *t* data pairs) that are independent of elapsed time for each controlled-potential electrolysis; these data points are spaced at equal time intervals such that data collection and storage occur at a constant frequency. If one wishes to integrate accurately the total charge for a given electrolysis, some regions of relatively high current at the beginning of an experiment may not be recorded, which results in an inaccurate integration (or an artificially low *n* value). In later work, we acquired and used PowerCORR®–2.47 software, which eliminates this problem.

All potentials in this paper are quoted with respect to a reference electrode consisting of a cadmium-saturated mercury amalgam in contact with DMF saturated with both cadmium chloride and sodium chloride; this electrode has a potential of −0.76 V versus the aqueous saturated calomel electrode (SCE) at 25 °C [22–24].

2.7. Identification and quantitation of electrolysis products

Upon completion of each controlled-potential (bulk) electrolysis, the catholyte was partitioned between diethyl ether and brine; the ether phase was washed with brine, dried over anhydrous sodium sulfate, and concentrated with the aid of rotary evaporation. An aliquot of the concentrated ether extract was injected into a Hewlett–Packard 5890 Series II gas chromatograph, equipped with an Agilent DB-5 capillary column (30 m × 0.32 mm × 0.25 μm film thickness) and a flame-ionization detector, to separate and quantitate the products obtained from the various electrolyses. An electroinactive internal standard (either *n*-nonane or *n*-dodecane) was added in known quantity before each solution was electrolyzed, and all product yields reported in this paper correspond to the absolute percentage of starting material incorporated into a particular species. Details about the procedures employed for the quantitation of products are described in a previous publication from our laboratory [25].

2.8. High-performance liquid chromatography–electrospray ionization–mass spectrometry (HPLC–ESI–MS)

To gain information about the identities of nickel(II) species before and after controlled-potential (bulk) electrolyses of solutions containing a large excess of 1-iodooctane, an Agilent 1100 capillary liquid chromatograph (Agilent Technologies, Wilmington, DE) was used. Samples (0.5 μL) taken before and after an electrolysis were injected onto a 0.5 mm i.d. × 150 mm long column packed with 5-μm Zorbax C18SB particles (Agilent). Eluent A was aqueous 1 mM ammonium acetate, and eluent B was 1 mM ammonium acetate in acetonitrile; these solutions were pumped at a flow rate of 15 μL min^{-1} with a solvent profile that began with 10% B at 0 min, followed by a linear gradient up to 95% B at 23 min and ended by a hold at 95% B for an additional 22 min to ensure that all species were eluted from the column prior to injection of the next sample. Detection and identification of the various nickel(II) complexes were accomplished by means of ultraviolet–visible absorption (254 nm) and electrospray ionization–mass spectrometry. A Perkin–Elmer Sciex API III mass spectrometer was used to record spectra of positive ions from *m*/*z* 200 to 900 every 3 s throughout the course of the chromatographic separation; the spray voltage was 3.85 kV and a sheath of nitrogen at 55 °C helped to desolvate the ions.

2.9. Liquid chromatography—ultraviolet–visible spectrophotometric analysis

A Varian ProStar liquid chromatography system including an autosampler (model 410), pump (model 230), and diode-array detector (model 335) equipped with an Alltech adsorbosphere HS C18 (250 mm × 4.6 mm, 5-μm particle size) and running Galaxie version 1.8.5005.5 software was used to separate and detect species in 50-μL samples of solutions obtained before and after controlled-potential electrolyses. Eluent A was 1 mM aqueous ammonium acetate, and eluent B was 1 mM ammonium acetate in acetonitrile. Mobile phase was pumped at 1 mL min^{-1} with an elution gradient that was 10% B at time 0, 10% B at 4 min, 100% B at 26.5 min, and held at 100% B for an additional 15 min.

3. Results and discussion

3.1. Cyclic voltammetric behavior of nickel(II) complexes

As depicted in Fig. 1, curve A, a cyclic voltammogram recorded at 100 mV s^{-1} reveals that the nickel(II) salen-nickel(I) salen redox couple behaves reversibly at a glassy carbon electrode in DMF containing 0.10 M $TBABF_4$; the cathodic peak potential (E_{pc}) is −0.96 V and the anodic peak potential (E_{pa}) is −0.88 V. These findings are in excellent agreement with observations made in an earlier investigation [26]. Under the same conditions, dimethylated nickel(II) salen, namely compound **3a**, exhibits reversible cyclic voltammetric behavior (Fig. 1, curve B), with the cathodic and anodic peak potentials, E_{pc} and E_{pa}, being −1.07 V and −0.99 V, respectively. Thus, the peak potentials for **3a** are displaced 110 mV toward more negative values with respect to those for nickel(II) salen. In additional experiments, we examined the cyclic voltammetric behavior of the two other analogues of nickel(II) salen—compounds **3b** and **3c**—synthesized in this work, and we observed as expected that each species undergoes a reversible one-electron reduction to its corresponding nickel(I) counterpart. Qualitatively, except for their positions along the potential axis, cyclic voltammograms for **3b** and **3c** are very similar in appearance to the curves seen in Fig. 1. A compilation of peak potentials for all four of the nickel(II) species is provided in Table 1. In addition, we found for each of the

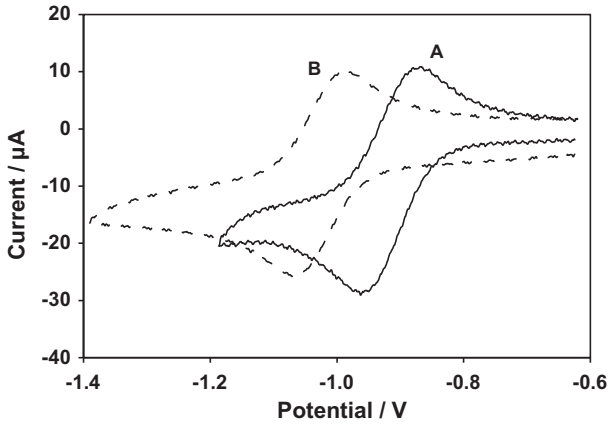

Fig. 1. Cyclic voltammograms recorded with a glassy carbon disk electrode (area = 0.077 cm^2) in oxygen-free DMF containing 0.10 M $TBABF_4$ at a scan rate of 100 mV s^{-1}: (A) 2.0 mM nickel(II) salen; (B) 2.0 mM **3a**. Note that E_{pc} and E_{pa} for **3a** are 110 mV more negative than the corresponding values for nickel(II) salen. Scans go from ca. −0.5 to −1.3 to −0.5 V.

Table 1
Cyclic voltammetric peak potentials and ΔE_{pc} values for 2.0 mM solutions of nickel(II) salen and substituted analogues obtained at 100 mV s^{-1} with a glassy carbon electrode in oxygen-free DMF containing 0.10 M $TBABF_4$.

Compound	Cathodic peak potential, E_{pc}/V[a]	Anodic peak potential, E_{pa}/V[a]	ΔE_{pc}/V[b]	
			Experimental	Theoretical
Nickel(II) salen	−0.96	−0.88		
3a	−1.07	−0.99	−0.11	−0.10
3b	−1.08	−1.00	−0.12	−0.14
3c	−0.96	−0.89	0.00	−0.03

[a] All potentials are given with respect to a cadmium-saturated mercury amalgam reference electrode, the potential of which is −0.76 V versus the aqueous saturated calomel electrode (SCE) at 25 °C; see text for additional information.
[b] ΔE_{pc} = [E_{pc} for substituted nickel(II) salen − E_{pc} for nickel(II) salen].

four complexes that the peak current ratio, I_{pc}/I_{pa}, for the nickel(II)–nickel(I) couple is very close to unity.

3.2. Computational studies of energy levels in nickel complexes

To probe the effects of alkyl or phenyl substituents on the electronic structures of the various nickel salen species, and to understand the accompanying shifts in their observed reduction potentials, we performed theoretical studies using density functional theory with the standard B3LYP functional [27,28]. We utilized the 6-31+G* basis set [29,30] containing a set of polarization functions (*f* for Ni, *d* for C, N, and O) as well as a set of diffuse functions (*spd* for Ni, *sp* for C, N, and O) to optimize the geometries of the parent as well as the substituted forms of neutral nickel(II) salen and the anionic forms of nickel(I) salen. Vibrational frequencies were calculated for the optimized structures and were used to determine zero-point vibrational corrections along with other thermodynamic quantities such as entropies and free energies. Single-point calculations were then carried out with a larger 6-311+G(2df) basis set [31,32] (roughly triple-zeta + diffuse functions + 2*f*, 1*g* on Ni, and 2*d*, 1*f* on C, N, and O) including solvation effects based on the SMD (Solvation Model Density-based) continuum model [33] (with 36.7 as the dielectric constant for DMF). All calculations were carried out with the aid of the Gaussian suite of electronic structure programs [34].

Listed in the final two columns of Table 1 are both experimental and theoretical values of ΔE_{pc}, expressed as the difference between E_{pc} for each of the three substituted nickel(II) salens and E_{pc} for nickel(II) salen itself. We believe that our findings show excellent quantitative agreement between experiment and theory. Our calculations indicate that the methyl and ethyl groups of **3a** and **3b**, respectively, shift E_{pc} in the negative direction by approximately 100 mV, whereas ΔE_{pc} for **3c** is rather small. These trends are consistent with the expectations from simple models based on how alkyl or phenyl substituents on the imino carbon atoms of the ligand should affect the electrochemical behavior of the various complexes. For example, since methyl groups are mildly electron donating, the electron density around the metal center of **3a** will be greater than that for nickel(II) salen itself, which makes it more difficult to add an electron to (or to reduce) **3a**. Another factor that may contribute to the observed substituent effect is that charge delocalization on the imino carbon will be less probable for electrogenerated dimethylated nickel(I) salen than for nickel(I) salen. For dimethylated nickel(I) salen, the imino carbon atom is tertiary, whereas the same position in nickel(I) salen is secondary; it is well known that carbanion stability is 1° > 2° > 3°. Therefore, dimethylated nickel(I) salen will not be resonance stabilized to the extent that nickel(I) salen is. Substituent effects arising from the larger ethyl group or from the phenyl group are also consistent with our expectations. For **3b** the electron-donating effect for the ethyl groups is expected to be larger than that for the methyl groups of **3a**, resulting in a slightly larger negative shift in E_{pc} for **3b**, as seen both experimentally and theoretically in Table 1. In the case of **3c**, the substituent effect due to the phenyl groups is expected to be smaller due to the presence of the sp^2 carbon; the perpendicular orientation of the phenyl groups with respect to the rest of the ligand suggests that electron delocalization effects are likely to play only a minor role.

Another interesting factor to consider for **3a–c** is the gap between the energy levels associated with metal- and ligand-centered one-electron reduction. In previous work [1], we showed that two low-energy orbitals are available for the reduction of nickel(II) salen—a metal-centered antibonding *d* orbital or a ligand-based orbital that is distributed across the aromatic rings with the largest amplitude on the imino carbon atoms. Calculations for the parent nickel salen [1] indicated that, although the metal-centered electronic state is more stable, only a small energy gap (2–3 kcal mol^{-1}) exists between the two orbitals, suggesting that it is possible to populate both electronic states. For the one-electron reductions of **3a–c,** the energy gap between the metal- and ligand-centered orbitals is even smaller, *although the metal-centered electronic state remains the ground state in all cases.*

Optimized ground-state structures for nickel(I) salen and the dimethyl-, diethyl-, and diphenyl-substituted nickel(I) complexes are consistent with the picture above. All of these nickel(I) salen species have C_2 symmetry, the ground state is ^2B in all cases, and all nickel–nitrogen and nickel–oxygen bond distances increase significantly (by 0.10–0.15 Å) relative to neutral nickel(II) salen, which is consistent with occupation of the antibonding *d* orbital. It is interesting that the shifts in E_{pc} seen in Table 1 for **3a–c** parallel the changes in the corresponding nickel–nitrogen bond lengths that arise from the methyl, ethyl, and phenyl substituents, though these changes are small in magnitude. For example, the changes in nickel–nitrogen bond lengths in the ground-state anions due to the methyl and ethyl substituents are similar, 0.005 and 0.006 Å, respectively, whereas the change in nickel–nitrogen bond length arising from the phenyl substituents is much smaller (0.001 Å). For all of the ground-state reduced anionic forms, inspection of the spin-densities obtained from a Mulliken population analysis reveals that the one-electron reduction occurs mostly on the nickel center, in accordance with the traditional picture for the nickel(I) salen species.

3.3. Cyclic voltammetric behavior of nickel(II) species in the presence of 1-iodobutane

In earlier work reported from our laboratory [12], we offered evidence that, during the catalytic reduction of alkyl halides by the reduced form of nickel(II) salen, the imino bonds of the ligand are alkylated by the organic moiety of the substrate. In addition, we demonstrated that (a) an alkylated nickel(II) salen species undergoes one-electron reduction at potentials more negative than does nickel(II) salen itself and (b) the alkylated, reduced form of nickel(II) salen can act as an effective catalyst for the reduction of alkyl halides [1]. To corroborate and extend these previous findings, cyclic voltammetry has been employed in the present investigation to examine and compare the electrochemical behavior of nickel(II) salen as well as compounds **3a–c** in the presence of 1-iodobutane. Accordingly, Figs. 2–5, respectively, display cyclic voltammograms for the reduction of nickel(II) salen and compounds **3a–c** at a glassy carbon cathode in a DMF–0.10 M $TBABF_4$ medium containing 1-iodobutane.

Fig. 2 shows cyclic voltammograms for the reduction of nickel(II) salen in the presence of four different concentrations of 1-iodobutane. As seen for curves B–E, the first cathodic peak, coming at a potential slightly more positive than that for reduction of nick-

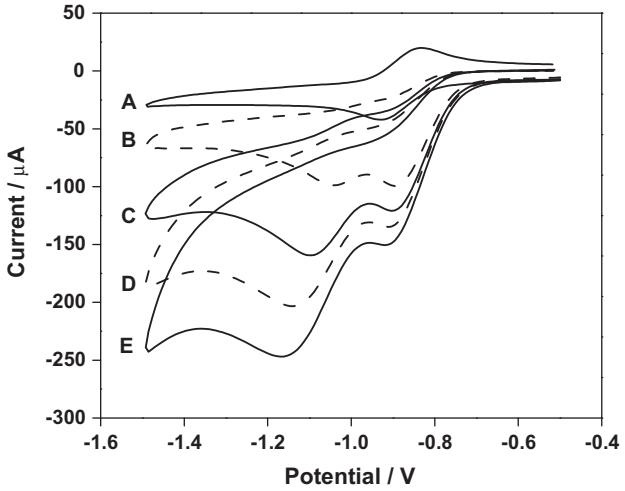

Fig. 2. Cyclic voltammograms recorded with a glassy carbon disk electrode (area = 0.077 cm^2) in oxygen-free DMF containing 0.10 M $TBABF_4$ at a scan rate of 100 mV s^{-1}: (A) 2.0 mM nickel(II) salen; (B) 2.0 mM nickel(II) salen and 5.0 mM 1-iodobutane; (C) 2.0 mM nickel(II) salen and 10.0 mM 1-iodobutane; (D) 2.0 mM nickel(II) salen and 15.0 mM 1-iodobutane; (E) 2.0 mM nickel(II) salen and 20.0 mM 1−iodobutane. Scans go from ca. −0.5 to −1.5 to −0.5 V.

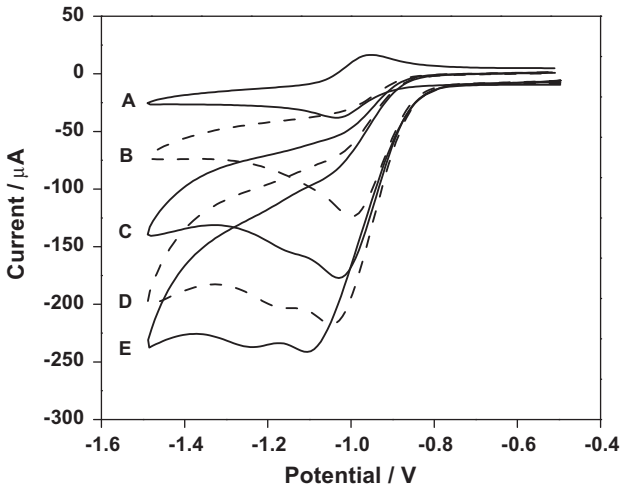

Fig. 3. Cyclic voltammograms recorded with a glassy carbon disk electrode (area = 0.077 cm^2) in oxygen-free DMF containing 0.10 M $TBABF_4$ at a scan rate of 100 mV s^{-1}: (A) 2.0 mM **3a**; (B) 2.0 mM **3a** and 5.0 mM 1-iodobutane; (C) 2.0 mM **3a** and 10.0 mM 1-iodobutane; (D) 2.0 mM **3a** and 15.0 mM 1-iodobutane; (E) 2.0 mM **3a** and 20.0 mM 1-iodobutane. Scans go from ca. −0.5 to −1.5 to −0.5 V.

el salen by itself (curve A), is attributable to catalytic cleavage of the carbon–iodine bond of the substrate; when the substrate concentration is increased, the magnitude of the first peak exhibits a nonproportional rise. As the concentration of 1-iodobutane is increased from 5.0 to 20.0 mM, a second cathodic peak becomes more and more prominent. It is proposed that this second peak is due to reduction of a butylated form of nickel(II) salen, for which one or more butyl moieties (arising from catalytic reduction of the alkyl iodide) have been added to the imino bonds of the salen ligand [1,12]. Mechanistic pathways for the production of butylated nickel(II) species are outlined in an earlier publication [1].

In Fig. 3, which pertains to the system involving **3a** and 1-iodobutane, catalytic cleavage of the carbon–iodine bond of the substrate is again evidenced by the shift of the first peak to slightly more positive potentials, similar to what is seen in Fig. 2, and the height of the first peak increases, though not linearly, as the concentration of 1-iodobutane is raised. More significant, however, is

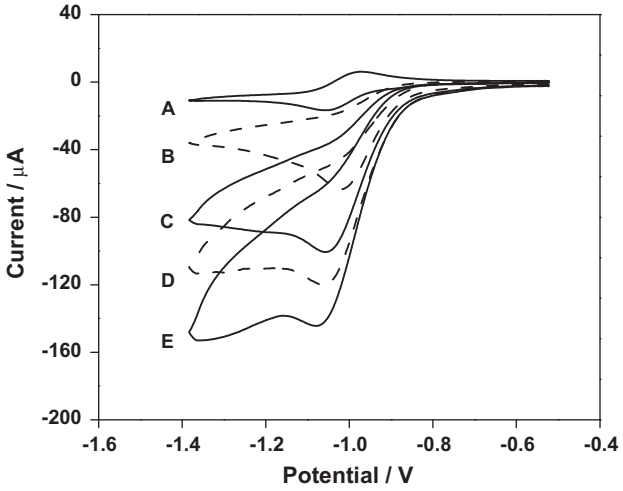

Fig. 4. Cyclic voltammograms recorded with a glassy carbon disk electrode (area = 0.077 cm^2) in oxygen-free DMF containing 0.10 M $TBABF_4$ at a scan rate of 100 mV s^{-1}: (A) 2.0 mM **3b**; (B) 2.0 mM **3b** and 5.0 mM 1-iodobutane; (C) 2.0 mM **3b** and 10.0 mM 1-iodobutane; (D) 2.0 mM **3b** and 15.0 mM 1-iodobutane; (E) 2.0 mM **3b** and 20.0 mM 1-iodobutane. Scans go from ca. −0.5 to −1.4 to −0.5 V.

the fact that the second cathodic peak is not apparent until the concentration of 1-iodobutane is five times larger than the concentration of **3a**. Even when the substrate concentration is 10 times that of **3a**, the second reduction peak is not as prominent as for any of the cyclic voltammograms in Fig. 2. This behavior can be explained by the fact that the methyl groups of **3a** sterically hinder butylation of the imino bonds, thereby diminishing the magnitude of the second cathodic peak.

Figs. 4 and 5, respectively, show cyclic voltammograms for the reduction of **3b** and **3c** in the presence of several concentrations of 1-iodobutane. Because the methyl and ethyl substituents are comparable in size, the trends seen for Fig. 4 are quite similar to those just described for Fig. 3. On the other hand, as revealed by Fig. 5, the presence of a much bulkier phenyl group on the carbon atom of each imino (C═N) bond of **3c** appears to block butylation of the ligand completely, since a second cathodic peak cannot be seen.

3.4. Use of high-performance liquid chromatography–electrospray ionization–mass spectrometry (HPLC–ESI–MS) to investigate alkylation of nickel complexes during controlled-potential (bulk) catalytic reductions of 1-iodooctane and 1-bromo-5-decyne

For earlier work carried out in our laboratory [12], high-performance liquid chromatography–electrospray ionization–mass spectrometry (HPLC–ESI–MS) was employed to separate and identify alkylated forms of nickel(II) salen produced during the catalytic reduction of several alkyl halides, and ^{1}H NMR spectrometry was used to establish the sites on the imino bonds of the salen ligand where alkylation takes place.

On the basis of the cyclic voltammetry experiments discussed in Section 3.3, it was anticipated that the sterically hindered dimethylated nickel(II) salen, namely compound **3a**, would not undergo alkylation of the imino bonds of the ligand to the same extent as nickel(II) salen itself. To test our expectation, we carried out controlled-potential (bulk) electrolyses involving the reduction of 1 mM solutions of either nickel(II) salen or **3a** at reticulated vitreous carbon cathodes held at −1.10 V in DMF–0.10 M $TBABF_4$ containing 40 mM 1-iodooctane. Before and after each electrolysis, HPLC–ESI–MS was used to determine and compare the extent of octylation of nickel(II) salen and **3a**.

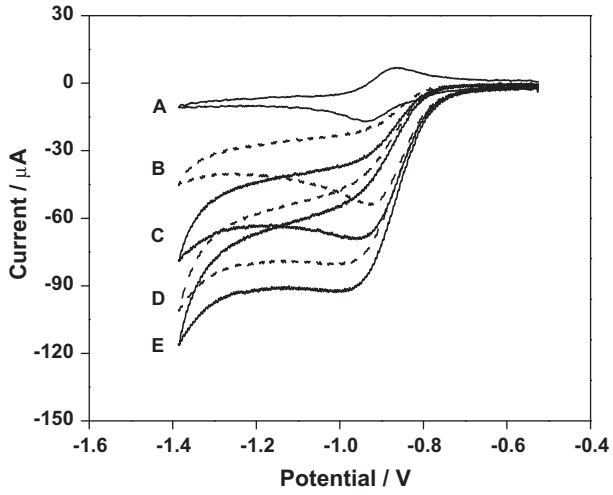

Fig. 5. Cyclic voltammograms recorded with a glassy carbon disk electrode (area = 0.077 cm^2) in oxygen-free DMF containing 0.10 M $TBABF_4$ at a scan rate of 100 mV s^{-1}: (A) 2.0 mM **3c**; (B) 2.0 mM **3c** and 5.0 mM 1-iodobutane; (C) 2.0 mM **3c** and 10.0 mM 1-iodobutane; (D) 2.0 mM **3c** and 15.0 mM 1-iodobutane; (E) 2.0 mM **3c** and 20.0 mM 1-iodobutane. Scans go from ca. −0.5 to −1.4 to −0.5 V.

Shown in Fig. 6A and B are pre- and post-electrolysis chromatograms for the nickel(II) salen–1-iodooctane system. Fig. 6A reveals a prominent peak associated with monoprotonated nickel(II) salen (*m*/*z* 325) at a retention time of 17.0 min and a smaller peak attributable to the monoprotonated, demetalated salen ligand (*m*/*z* 269) at 28.3 min. Fig. 6B, obtained after a controlled-potential electrolysis, clearly demonstrates the change in the amount of unmodified nickel(II) salen, as evidenced by the dramatic decrease in the intensity of the peak at 17.0 min as well as the appearance of a new, major peak at 23.0 min that was identified with the aid of ESI–MS to correspond to monoprotonated, monooctyl nickel(II) salen (*m*/*z* 439) along with a small amount of what is believed to be the monoprotonated dimer of monooctyl nickel(II) salen (*m*/*z* 877). Thus, as reported previously [12], an unprotected imino carbon atom of the salen ligand is prone to substitution by an octyl moiety arising from the nickel(I) salen-catalyzed reduction of 1-iodooctane.

As seen from the pre- and post-electrolysis chromatograms in Fig. 6C and D, the **3a**–1-iodooctane system exhibits behavior significantly different from that of the nickel(II) salen–1-iodooctane system. Fig. 6C shows a pre-electrolysis chromatogram with a peak due to monoprotonated **3a** (*m*/*z* 353) at 17.5 min and another peak attributable to the monoprotonated, demetalated ligand, **2a**, (*m*/*z* 297) at 28.3 min. However, after a controlled-potential electrolysis, the decrease in the size of the peak at 17.5 min (Fig. D) is much less than that for the nickel(II) salen–1-iodooctane system (Fig. 6B). Moreover, there is almost no signal at all due to monoprotonated, monooctylated **3a** (*m*/*z* 467) at 23.9 min. These findings support the conclusion that the presence of methyl groups on the imino carbon atoms enhances the fidelity of the catalyst by suppressing octylation of the ligand.

Another set of HPLC–ESI–MS experiments focused on a comparison of the nickel(I) salen- or dimethylated nickel(I) salen-catalyzed electroreductive cyclization of 1-bromo-5-decyne, which affords pentylidenecyclopentane as the principal product [35]. We were interested in seeing (i) whether a 5-decyn-1-yl moiety derived from the parent acetylenic halide would be added to an imino bond of nickel(II) salen and (ii) whether the presence of a methyl group on the carbon atom of each imino bond of **3a** would prevent the addition of a 5-decyn-1-yl moiety onto the ligand. Accordingly, we performed controlled-potential electrolyses of 1 mM solutions of either nickel(II) salen or **3a** at reticulated vitreous carbon cathodes held at −1.10 V in DMF–0.10 M $TBABF_4$ containing 40 mM 1-bromo-5-decyne. As predicted, the post-electrolysis chromatogram for the experiment involving nickel(II) salen showed the presence of mostly unmodified monoprotonated nickel(II) salen (*m*/*z* 325) along with a small amount of monoprotonated nickel(II) salen with one 5-decyn-1-yl group bound to an imino carbon atom of the ligand (*m*/*z* 464). Furthermore, the post-electrolysis chromatogram for the experiment involving **3a** showed only a signal for monoprotonated **3a** (*m*/*z* 353) and no evidence at all for monoprotonated **3a** with an attached 5-decyn-1-yl group.

3.5. Controlled-potential (bulk) electrolyses of nickel(II) complexes; catalytic reductions of alkyl and acetylenic halides by electrogenerated dimethylated nickel(I) salen

Exhaustive bulk electrolyses of nickel(II) salen and of **3a–c** at reticulated vitreous carbon cathodes held at −1.10 V in 0.10 M $TMABF_4$–DMF yielded the following coulometric *n* values: (a) nickel(II) salen, *n* = 1.02; (b) **3a**, *n* = 1.07; (c) **3b**, *n* = 1.08; (d) **3c**, *n* = 1.10. On the basis of prior knowledge of the electrochemistry of nickel(II) salen and the cyclic voltammograms shown in Figs. 1–5, it is clear that reduction of each nickel(II) complex is a reversible, one-electron process.

Controlled-potential (bulk) electrolyses were conducted in which 1.0 mM solutions of **3a** in DMF–0.10 M $TMABF_4$ were reduced at reticulated vitreous carbon cathodes held at −1.10 V in the presence of either 1-bromo- or 1-iodooctane. Compiled in Table 2 are average results acquired from at least duplicate experiments for each concentration of alkyl halide. Coulometric *n* values (based on the initial concentration of alkyl halide) were essentially 1 for all electrolyses, and the products were identified and quantitated with the aid of GC and GC–MS. It is clear from the tabulated data that catalytic reduction of either 1-bromo- or 1-iodooctane leads predominantly to the production of a dimer (hexadecane), and that octane and 1-octene arise in relatively small yields either via disproportionation of octyl radicals or via abstraction of a hydrogen atom from the solvent by an octyl radical. It is interesting to compare the results of the present investigation (Table 2) for which **3a** served as the catalyst precursor with the results obtained in earlier work [12] for which unsubstituted nickel(II) salen was employed as the catalyst precursor. As a part of each of these studies, reduction of a 10.0 mM solution of 1-bromo- or 1-iodooctane was carried out in the presence of a 1.0 mM concentration of electrogenerated catalyst; in both instances, hexadecane was the principal product, and octane and 1-octene were minor species. However, when unsubstituted nickel(II) salen was used as the catalyst precursor, more than 20% of the original 1-bromo- or 1-iodooctane was lost due to octylation of the ligand [12]. On the other hand, when **3a** served as the catalyst precursor, at least 98% of the initial alkyl halide was converted into hydrocarbon products (Table 2), because the presence of a methyl group on the carbon atom of each imino bond strongly suppresses octylation of the ligand. This is further proof that placing appropriate substituents on the salen ligand prevents alkylation of the imino bonds and improves dramatically the total recovery of desired products.

In previous work performed in our laboratory, we demonstrated that carbocyclic compounds are produced via the nickel(I) salen-catalyzed reductions of acetylenic halides [9,35,36]. Accordingly, it was of interest to establish whether electrogenerated dimethylated nickel(I) salen can serve as an effective catalyst for the reductive intramolecular cyclizations of 1-bromo- and 1-iodo-5-decyne. Listed in Table 3 are the results of controlled-potential (bulk) electrolyses of 1 mM solutions of **3a** in the presence of either 1-bromo- or 1-iodo-5-decyne carried out in 0.10 M $TMABF_4$–DMF at reticulated vitreous carbon cathodes held at −1.10 V. Each entry

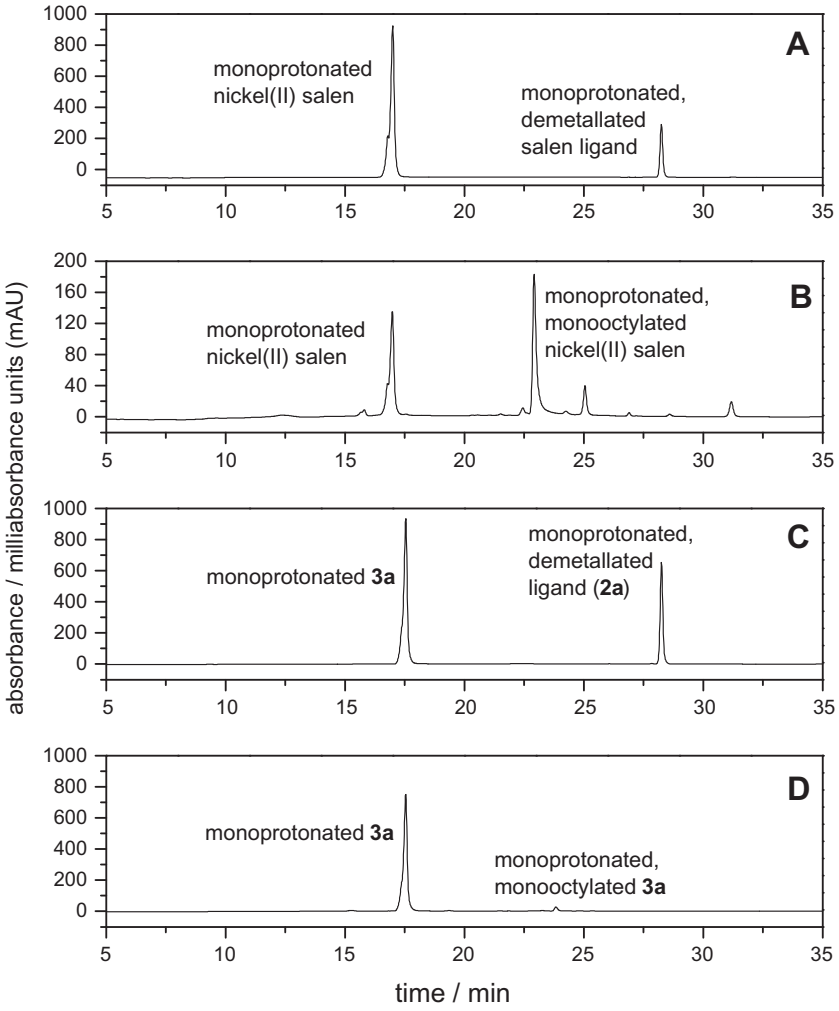

Fig. 6. Chromatograms showing the extent of octylation of nickel(II) salen and of **3a** before and after controlled-potential (bulk) electrolyses at reticulated vitreous carbon cathodes held at −1.10 V in DMF–0.10 M $TBABF_4$ containing an excess of 1-iodooctane: (A) pre-electrolysis chromatogram of a solution containing 1.0 mM nickel(II) salen and 40.0 mM 1-iodooctane, (B) post-electrolysis chromatogram of a solution originally containing 1.0 mM nickel(II) salen and 40.0 mM 1-iodooctane, (C) pre-electrolysis chromatogram of a solution containing 1.0 mM **3a** and 40.0 mM 1-iodooctane, and (D) post-electrolysis chromatogram of a solution originally containing 1.0 mM **3a** and 40.0 mM 1-iodooctane. Chromatograms are plotted as absorbance at 254 nm (in milliabsorbance units, mAU) versus separation time (in min).

Table 2
Product distributions and coulometric *n* values for controlled-potential (bulk) electrolyses of 1 mM solutions of **3a** at reticulated vitreous carbon cathodes held at −1.10 V in DMF containing 0.10 M $TMABF_4$ and either 1-iodooctane or 1-bromooctane.

Substrate	Concentration (mM)	n[b]	Product distribution (%)[a]			
			8	**9**	**10**	Total
1-Iodooctane	10	1.01	4	9	87	100
1-Iodooctane	20	0.93	4	7	82	93
1-Iodooctane	40	1.04	3	16	82	101
1-Bromooctane	10	0.92	5	4	89	98
1-Bromooctane	20	0.92	3	3	83	89

8 = Octane; **9** = 1-octene; **10** = hexadecane.
[a] Yield expressed as absolute percentage of substrate converted to product.
[b] Average number of electrons per molecule of substrate.

Table 3
Product distributions and coulometric *n* values for controlled-potential (bulk) electrolyses of 1 mM solutions of **3a** at reticulated vitreous carbon cathodes held at −1.10 V in DMF containing 0.10 M $TMABF_4$ and either 1-bromo-5-decyne or 1-iodo-5-decyne.

Substrate	Concentration (mM)	n[b]	Product distribution (%)[a]			
			13a	**14a**	**15a**	Total
1-Bromo-5-decyne	5	0.90	11	3	74	88
1-Bromo-5-decyne	10	0.93	10	4	74	88
1-Iodo-5-decyne	5	0.97	8	3	88	99
1-Iodo-5-decyne	10	0.95	11	4	82	97

13a = Dec-5-yne; **14a** = dec-1-en-5-yne; **15a** = pentylidenecyclopentane.
[a] Yield expressed as absolute percentage of substrate converted to product.
[b] Average number of electrons per molecule of substrate.

in Table 3 represents the average of several experiments; for each of the electrolyses, the coulometric *n* value was essentially 1. As expected, the principal product is the desired carbocycle (pentylidenecyclopentane), which is obtained in greater than 70% yield, whereas straight-chain species (dec-5-yne and dec-1-en-5-yne) are formed in no higher than 11% yield. These findings are comparable to those previously reported [35] when electrogenerated nickel(I) salen is used as catalyst. Although a dimeric product (icosa-5,15-diyne) was obtained in our earlier work [35] with electrogenerated nickel(I) salen, this compound was not detected in the present investigation, undoubtedly because a lower concentration of substrate was utilized (Table 3), thereby diminishing the bimolecular coupling of primary alkyl radicals.

A final series of experiments involved the electroreduction of **3a** in the presence of a phenyl-conjugated acetylenic halide (6-bromo-

1-phenyl-1-hexyne) to ascertain if electroreductive intramolecular cyclization of the substrate can be catalytically induced. In all other respects, these electrolyses were carried out as described in the preceding paragraph; the initial concentration of **3a** was 1 mM and that of 6-bromo-1-phenyl-1-hexyne was either 5 or 10 mM. For duplicate experiments involving 5 mM substrate, the average *n* value was 1.01, and the products were benzylidenecyclopentane (89%), (cyclopentenylmethyl)benzene (8%), and 1-phenyl-1-hexyne (formed in barely detectable amounts); for duplicate electrolyses with 10 mM substrate, the average *n* value was 0.93, and the products were benzylidenecyclopentane (83%), (cyclopentenylmethyl)benzene (12%), and 1-phenyl-1-hexyne (in trace quantities). When these results are compared with those obtained with electrogenerated nickel(I) salen as a catalyst [36], some differences can be noted, although benzylidenecyclopentane is produced in similar yields with either of the two catalysts. When 6-bromo-1-phenyl-1-hexyne is catalytically reduced with dimethylated nickel(I) salen, (cyclopentenylmethyl)benzene and 1-phenyl-1-hexyne are formed as minor products, whereas 1-phenyl-1-hexyne (13–16%) is the sole minor product obtained when electrogenerated nickel(I) salen is the catalyst. In view of the differences encountered when acetylenic halides are catalytically reduced by either

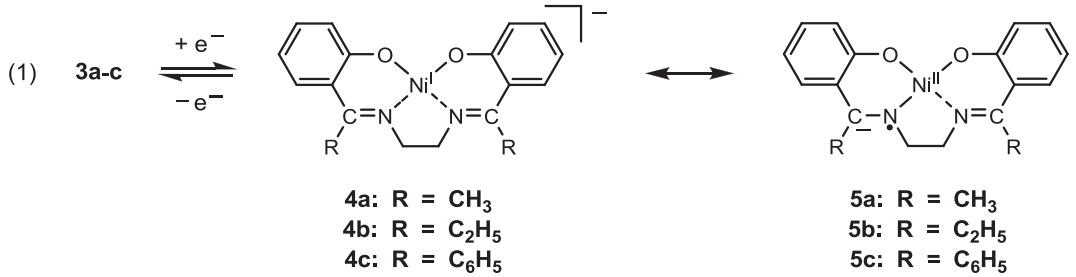

(2) **4a-c** (or **5a-c**) + $C_8H_{17}X$ (**6**) → **3a-c** + $C_8H_{17}^{\bullet}$ (**7**) + X^-

(3) **7** + SH → C_8H_{18} (**8**) + $S^{\bullet}$

(4) 2 **7** → **8** + $C_6H_{13}CH{=}CH_2$ (**9**)

(5) 2 **7** → $C_{16}H_{34}$ (**10**)

(6) **4a-c** (or **5a-c**) + $R'C{\equiv}C(CH_2)_4X$ → **3a-c** + $R'C{\equiv}C(CH_2)_4^{\bullet}$ + X^-

11a: R' = C_4H_9
11b: R' = C_6H_5

12a: R' = C_4H_9
12b: R' = C_6H_5

(7) **12a** (or **12b**) + SH → $R'C{\equiv}CC_4H_9$ + $S^{\bullet}$

13a: R' = C_4H_9
13b: R' = C_6H_5

(8) 2 **12a** → **13a** + $R'C{\equiv}C(CH_2)_2CH{=}CH_2$

14a: R' = C_4H_9

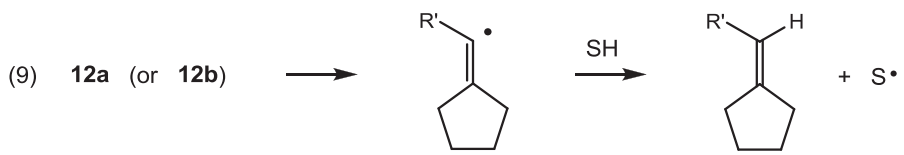

15a: R' = C_4H_9
15b: R' = C_6H_5

Scheme 1.

electrogenerated nickel(I) salen or dimethylated nickel(I) salen, it should be of future interest to explore both the electrosynthetic and mechanistic implications of these results in more detail.

3.6. Mechanistic features of the catalytic reduction of alkyl and acetylenic halides by electrogenerated nickel(I) complexes

Depicted in Scheme 1 is a sequence of mechanistic steps that are compatible with observations made in this investigation, that serve to rationalize the differences in the behavior of **3a**–**c** in comparison with nickel(II) salen itself, and that can account for products arising from catalytic reduction of various alkyl and acetylenic halides.

Reaction (1) shows the one-electron reductions of **3a**–**c** to give either a metal-reduced species (**4a**–**c**) or a ligand-reduced species (**5a**–**c**). Electrogenerated **4a**–**c** and **5a**–**c** quickly transfer an electron to a primary alkyl halide, such as 1-bromo- or 1-iodooctane (**6**), cleaving the carbon–halogen bond to produce a reactive radical intermediate (**7**), along with a free halide ion, and to regenerate **3a**–**c** (Reaction (2)). Once formed, radical **7** can abstract a hydrogen atom from the solvent (SH) to afford an alkane (**8**) (Reaction (3)), can disproportionate to yield an alkane and an alkene (**9**) (Reaction (4)), or can undergo coupling to give a dimeric product (**10**) (Reaction (5)).

In analogous fashion, an acetylenic halide (**11a** or **11b**) is reduced by either **4a–c** or **5a–c** to give a primary radical (**12a** or **12b**) (Reaction (6)) that, as shown in Reaction (7), abstracts a hydrogen atom from the solvent to form an alkyne (**13a** or **13b**). In addition, radical **12a** can disproportionate to yield an alkyne (**13a**) and an alkenyne (**14a**) (Reaction (8)), and radicals **12a** and **12b** can each cyclize intramolecularly, followed by hydrogen-atom abstraction from the solvent, to afford a carbocyclic product (**15a** or **15b**) (Reaction (9)).

One product obtained from the catalytic reduction of 6-bromo-1-phenyl-1-hexyne by electrogenerated dimethylated nickel(I) salen that is not accounted for in Scheme 1 is (cyclopentenylmethyl)benzene. This species was encountered in an earlier study [19] of the electroreductive intramolecular cyclization of 6-chloro-1-phenyl-1-hexyne at a mercury cathode in DMF containing 0.10 M tetra-*n*-butylammonium perchlorate; for that system, the acetylenic chloride was proposed to undergo base-catalyzed isomerization to 6-chloro-1-phenyl-1,2-hexadiene, with the latter phenyl-conjugated allene being reduced to a radical–anion which cyclizes with expulsion of chloride ion to afford a cyclic allyl radical that can be further reduced and then protonated by the medium to give either benzylidenecyclopentane or (cyclopentenylmethyl)benzene. In the present investigation, several pathways leading to (cyclopentenylmethyl)benzene can be proposed. First, it is conceivable that benzylidenecyclopentane (**15b**) donates a hydrogen atom to a solvent-derived radical ($S^{\cdot}$) to form an allylic radical which, upon rearrangement and reabstraction of a hydrogen atom from the solvent, affords (cyclopentenylmethyl)benzene. Second, some 6-bromo-1-phenyl-1-hexyne might experience a fate similar to that described in the preceding paragraph. Third, the radical precursor of benzylidenecyclopentane shown in Reaction (9) might undergo one-electron reduction, followed by rearrangement and protonation, to give (cyclopentenylmethyl)benzene. Fourth, benzylidenecyclopentane might be involved in a base-induced isomerization to form (cyclopentenylmethyl)benzene. However, the last three alternatives involve carbanionic intermediates the formation of which requires extra coulombs of electricity—an event that is not compatible with observed coulometric *n* values.

Acknowledgments

High-resolution mass analyses were performed in the Indiana University Mass Spectrometry Facility; the HRMS system was purchased with funds provided by the National Institutes of Health Grant No. 1S10RR016657-01. This work was supported in part by Department of Energy Grant No. DE-FG02-07ER15889 to K.R.

References

[1] P.W. Raess, M.S. Mubarak, M.A. Ischay, M.P. Foley, T.B. Jennermann, K. Raghavachari, D.G. Peters, J. Electroanal. Chem. 603 (2007) 124.
[2] E. Duñach, A.P. Esteves, M.J. Medeiros, S. Olivero, Green Chem. 8 (2006) 380.
[3] E. Duñach, M.J. Medeiros, Electrochim. Acta 53 (2008) 4470.
[4] A.P. Esteves, C.S. Neves, M.J. Medeiros, D. Pletcher, J. Electroanal. Chem. 614 (2008) 131.
[5] A.P. Esteves, E.C. Ferreira, M.J. Medeiros, Tetrahedron 63 (2007) 3006.
[6] E. Duñach, A.P. Esteves, M.J. Medeiros, C.S. dos Santos Neves, S. Olivero, C. R. Chimie 12 (2009) 889.
[7] X. Chaminade, E. Duñach, A.P. Esteves, M.J. Medeiros, C.S. Neves, S. Olivero, Electrochim. Acta 54 (2009) 5120.
[8] E. Duñach, M.J. Medeiros, S. Olivero, New J. Chem. 30 (2006) 1534.
[9] M.S. Mubarak, T.B. Jennermann, M.A. Ischay, D.G. Peters, Eur. J. Org. Chem. (2007) 5346.
[10] M.S. Mubarak, W.E. Barker IV, D.G. Peters, J. Electrochem. Soc. 154 (2007) F205.
[11] J.A. Miranda, C.J. Wade, R.D. Little, J. Org. Chem. 70 (2005) 8017.
[12] D.M. Goken, M.A. Ischay, D.G. Peters, J.W. Tomaszewski, J.A. Karty, J.P. Reilly, M.S. Mubarak, J. Electrochem. Soc. 153 (2006) E71.
[13] C. Gosden, K.P. Healy, D. Pletcher, J. Chem. Soc., Dalton Trans. (1978) 972.
[14] J.K. Crandall, D.J. Keyton, Tetrahedron Lett. (1969) 1653.
[15] J.K. Crandall, W.J. Michaely, J. Organomet. Chem. 51 (1973) 375.
[16] R. Shao, J.A. Cleary, D.M. La Perriere, D.G. Peters, J. Org. Chem. 48 (1983) 3289.
[17] B.C. Willett, W.M. Moore, A. Salajegheh, D.G. Peters, J. Am. Chem. Soc. 101 (1979) 1162.
[18] W.J. Michaely, Ph.D. Thesis, Indiana University, Bloomington, IN, 1971.
[19] W.M. Moore, A. Salajegheh, D.G. Peters, J. Am. Chem. Soc. 97 (1975) 4954.
[20] K.L. Vieira, D.G. Peters, J. Electroanal. Chem. 196 (1985) 93.
[21] J.A. Cleary, M.S. Mubarak, K.L. Vieira, M.R. Anderson, D.G. Peters, J. Electroanal. Chem. 198 (1986) 107.
[22] L.W. Marple, Anal. Chem. 39 (1967) 844.
[23] C.W. Manning, W.C. Purdy, Anal. Chim. Acta 51 (1970) 124.
[24] J.L. Hall, P.W. Jennings, Anal. Chem. 48 (1976) 2026.
[25] W.A. Pritts, K.L. Vieira, D.G. Peters, Anal. Chem. 65 (1993) 2145.
[26] A.L. Butler, D.G. Peters, J. Electrochem. Soc. 144 (1997) 4212.
[27] A.D. Becke, J. Chem. Phys. 98 (1993) 5648.
[28] C.T. Lee, W.T. Yang, R.G. Parr, Phys. Rev. B 37 (1988) 785.
[29] P.C. Hariharan, J.A. Pople, Theor. Chem. Acc. 28 (1973) 213.
[30] V.A. Rassolov, J.A. Pople, M.A. Ratner, T.L. Windus, J. Chem. Phys. 109 (1998) 1223.
[31] R. Krishnan, J.S. Binkley, R. Seeger, J.A. Pople, J. Chem. Phys. 72 (1980) 650.
[32] K. Raghavachari, G.W. Trucks, J. Chem. Phys. 91 (1989) 1062.
[33] A.V. Marenich, C.J. Cramer, D.G. Truhlar, J. Phys. Chem. B 113 (2009) 6378.
[34] Gaussian 09, Revision A.02, M.J. Frisch, G.W. Trucks, H.B. Schlegel, G.E. Scuseria, M.A. Robb, J.R. Cheeseman, G. Scalmani, V. Barone, B. Mennucci, G.A. Petersson, H. Nakatsuji, M. Caricato, X. Li, H.P. Hratchian, A.F. Izmaylov, J. Bloino, G. Zheng, J.L. Sonnenberg, M. Hada, M. Ehara, K. Toyota, R. Fukuda, J. Hasegawa, M. Ishida, T. Nakajima, Y. Honda, O. Kitao, H. Nakai, T. Vreven, J.A. Montgomery, Jr., J.E. Peralta, F. Ogliaro, M. Bearpark, J.J. Heyd, E. Brothers, K.N. Kudin, V.N. Staroverov, R. Kobayashi, J. Normand, K. Raghavachari, A. Rendell, J.C. Burant, S.S. Iyengar, J. Tomasi, M. Cossi, N. Rega, J.M. Millam, M. Klene, J.E. Knox, J.B. Cross, V. Bakken, C. Adamo, J. Jaramillo, R. Gomperts, R.E. Stratmann, O. Yazyev, A.J. Austin, R. Cammi, C. Pomelli, J.W. Ochterski, R.L. Martin, K. Morokuma, V.G. Zakrzewski, G.A. Voth, P. Salvador, J.J. Dannenberg, S. Dapprich, A.D. Daniels, Ö. Farkas, J.B. Foresman, J.V. Ortiz, J. Cioslowski, D.J. Fox, Gaussian, Inc., Wallingford CT, USA, 2009.
[35] M.A. Ischay, M.S. Mubarak, D.G. Peters, J. Org. Chem. 71 (2006) 623.
[36] M.S. Mubarak, D.G. Peters, J. Electroanal. Chem. 332 (1992) 127.